

## **Modeling of Geothermometer: How to develop Geothermometric Formulations of Selected Mineral Reactions**

**Lee, Han Yeang**

**Korea Institute of Geoscience and Mineral Resources(KIGAM)**

### **INTRODUCTION**

With the availability of many experimental phase-equilibrium studies and thermochemical data on several important silicates, geothermometric applications of mineralogic reactions have proliferated. In the coming years, there will be significant progress both in thermodynamic formulations of geothermometers and in the availability of thermochemical data. In this paper methods of development of garnet-orthopyroxene geothermometer from experimental works and available thermochemical data are introduced for understanding how to formulate this geothermometer.

### **EXPERIMENTAL METHODS**

The equilibrium  $K_D(\text{Fe-Mg})$  between garnet and orthopyroxene is approached from two directions, using high  $K_D$  and low  $K_D$  starting mixtures, at any given P and T, as in all classical reversal experiments which can provide the most unambiguous approach for the investigation of equilibrium compositions of coexisting minerals. In the high  $K_D$  starting mixtures, Mg-rich orthopyroxene is made to react with Fe-rich garnet, whereas in the low  $K_D$  starting mixture, Fe-rich orthopyroxene with garnet of comparable composition is used.

#### **Apparatus, Sample Configurations and P-T Measurements**

All experiments were carried out in an end-loaded Piston-Cylinder apparatus, using 1/2, 3/4 or 1 inch carbide-core pressure vessels and carbide pistons.

NaCl or CsCl were used as sleeves around graphite furnaces in the pressure cell(Fig.1) in a manner suggested by Boettcher et al.(1981), which greatly reduced the distortion of the furnace due to differential compression of pressure cell materials. No correction was made to the nominal pressure as salt sleeves offer very little frictional resistance to pressure(Mirwald et al., 1975). CsCl has a much lower thermal conductivity than NaCl, and thus helps reduce fracturing of the carbide cores due to thermal stress in relatively high P-T runs(Elphicks et al., 1985). The pressure cells were wrapped with 0.002 inch thick lead foil, and the inner wall of the pressure core was coated with hydrogen free 'Molykote'(MoS<sub>2</sub>) lubricant to reduce friction at high pressures. All pressure cells were dried in an oven at least for 12 hours at 150 °C before loading inside a pressure vessel. Samples were packed inside spectrographic quality graphite disks-each hole being tightly fitted with a graphite lid.

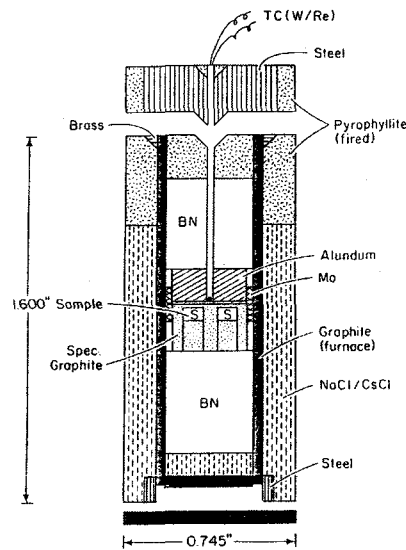


Fig. 1 Schematic illustration of the cross section of a typical pressure cell used in the experiments in Piston-Cylinder apparatus

Temperatures were measured with W3 per cent Re-W25 per cent Re thermocouples and encased in 99.99 per cent  $\text{Al}_2\text{O}_2$  ceramic tubings. The W-Re thermocouple is known to have superior mechanical and chemical stability, compared to Chromel-alumel and Pt-Rh thermocouples. To minimize thermocouple 'poisoning' by reaction with pressure cell material, a 0.015-0.020 inch alundum(99.99 per cent  $\text{Al}_2\text{O}_2$ ) disk was placed between the thermocouple junction and the top surface of the graphite container. The thermocouple junction was 0.050 inch from the sample. The thickness of the sample disk within a graphite container was within 0.12 inch. Following Elphick et al.(1985) the graphite container was surrounded by a 0.20 inch high Mo ring, which was shorted to the furnace. The central sections of the furnace and Mo ring coincided with the top surface of the sample disk. This configuration reduced the temperature difference between the thermocouple junction and the lower surface of the sample disk to within  $5^\circ\text{C}$ (Elphick et al., 1985). The nominal temperatures were corrected for the pressure effect on the e.m.f. of W/Re thermocouple according to the method /discussed by Lane & Ganguly(1980). The corrected temperatures are 6-9 $^\circ\text{C}$  higher than the nominal ones. From our earlier experience with the problem of thermocouple stability in this type of pressure cell(e.g., Elphick et al., 1985), we believe that the true sample temperature for any run above 1200 $^\circ\text{C}$  was within  $\pm 10^\circ\text{C}$  of that reported for the run. The precision of temperature measurement is better at lower temperatures.

After the pressure cell is taken to the desired nominal run pressure at room temperature, it is left overnight to allow the cell to relax. Usually the pressure would drop by about 2-3 Kb on the following day, but the pressure builds up again by the thermal expansion of the pressure cells and of the oil which drives the rams. Generally fluctuations of several hundred bars are common during a run. However, if the pressure increases too much(2 Kb), it is adjusted manually by releasing the oil pressure. These fluctuations are the main source of uncertainties in the nominal run pressures as shown in Table 2.

### Starting Materials

Natural and synthetic garnet and orthopyroxene were used to prepare starting materials for studying the equilibrium compositions of coexisting garnet and orthopyroxene. Natural

samples with  $X_{Fe} + X_{Mg} = 0.97$  were separated from various rocks and handpicked under binocular microscope. The compositions of starting materials are given in Table 1.

**Table 1** Microprobe analysis of starting materials.

	Orthopyroxenes					Garnet		
	Opx/ 1	Opx/ 2	Opx/ 3	Opx/ 4	Opx/ 5	Gt/ 1	Gt/ 2	Gt/ 3
FeO <sup>+</sup>	9.32	46.76	31.14	-	34.86	35.37	22.74	0.04
MgO	33.81	5.09	17.80	37.77	13.55	5.34	13.01	29.80
SiO <sub>2</sub>	56.30	47.57	51.79	56.62	50.28	38.48	39.18	44.95
Al <sub>2</sub> O <sub>3</sub>	0.08	0.75	0.07	6.43	0.03	21.33	23.25	25.74
CaO	0.32	0.61	-	-	0.58	0.40	1.80	0.19
MnO	0.05	0.05	-	-	1.30	0.03	0.49	-
Cr <sub>2</sub> O <sub>3</sub>	-	0.01	-	-	-	-	-	-
TiO <sub>2</sub>	-	0.02	-	-	-	0.02	-	-
Na <sub>2</sub> O	-	0.03	-	-	-	0.05	0.02	-
NiO	0.05	-	-	-	0.07	-	-	-
K <sub>2</sub> O	-	-	-	-	-	-	-	-
Total	99.94	100.90	100.70	100.82	100.68	101.09	100.40	100.72
Fe	0.545	3.260	1.999	-	2.306	2.322	1.424	0.002
Mg	3.529	0.635	2.037	3.734	1.597	0.624	1.452	2.960
Si	3.942	3.966	3.976	3.755	3.975	3.021	2.934	2.994
Al	0.006	0.074	0.006	0.502	0.002	1.973	2.051	2.020
Ca	0.023	0.054	-	-	0.049	0.040	0.144	0.013
Mn	0.003	0.003	-	-	0.086	0.001	0.031	-
Cr	-	-	-	-	-	-	-	-
Ti	-	-	-	-	-	0.001	-	-
Na	-	0.004	-	-	-	0.007	0.003	-
Ni	0.002	-	-	-	-	-	-	-
K	-	-	-	-	-	-	-	-
Cation Total	8.050	7.996	8.018	8.091	8.015	7.989	8.039	7.989
O : 12								
Fe/Mg	0.154	5.154	0.981	0.000	1.443	3.717	0.980	0.000
Fe/Fe+Mg	0.133	0.837	0.495	0.000	0.590	0.788	0.495	0.000

Opx/ 1 : Sample from Telmark, Norway(UCLA Mineral Museum)

Opx/ 2 : Sample No. XYZ, Ramberg and Devore(1951)

Opx/ 3 : Synthetic sample

Opx/ 4 : Synthetic sample

Opx/ 5 : Sample No. 5, Burtler

Gt/ 1 : Natural sample, Schneider Co.

Gt/ 2 : Natural sample No. 143895, Smithsonian Collection

Gt/ 3 : Synthetic pyrope

\*All iron assumed to be FeO

## Pyrope

Pyrope was synthesized hydrothermally in a sealed gold capsule from a stoichiometric mixture of reagent grade MgO, SiO<sub>2</sub>, and Al<sub>2</sub>O<sub>3</sub> at 25 Kb, 1000°C for 24 hours. The X-ray diffraction pattern showed single phase pyrope.

## Non-aluminous orthopyroxene

Non-aluminous orthopyroxene was synthesized from a mixture of reagent grade MgO, Fe<sub>2</sub>O<sub>3</sub>, and SiO<sub>3</sub>

under dry conditions in a graphite capsule at 25 Kb, 1200°C for 48 hours. The run product consisted of grains 200 $\mu$ m or larger. The average Fe/(Fe + Mg) ratio of the run product was 0.49 compared to the intended ratio of 0.6 of the starting material. Alloying of Fe with the graphite capsule (and weighing error) might have been responsible for the lower concentration of Fe in the run product. However, The X-ray diffraction pattern showed single phase orthopyroxene.

#### **Aluminous orthopyroxene**

Aluminous orthopyroxene was synthesized hydrothermally in a sealed gold capsule from a mixture of reagent grade MgO, Al<sub>2</sub>O<sub>3</sub>, and SiO<sub>2</sub> at 20 Kb, 1100°C for 48 hours. The mixture was seeded with 5 wt. per cent of synthetic aluminous enstatite (12 wt. per cent Al<sub>2</sub>O<sub>3</sub>) which was synthesized from an oxide mixture with 5 wt. per cent of natural pyroxene, Opx/ I (Table 1). The run product showed broad X-ray reflections implying significant in-homogeneity in the concentration of Al<sub>2</sub>O<sub>3</sub>. To improve homogeneity, the run product was crushed and recycled at 25 Kb, 1350°C for 48 hours in a dry graphite container. The X-ray peaks of the recycled product were sharper, and microprobe analyses of several grains yielded an average Al<sub>2</sub>O<sub>3</sub> content of 6.5 wt. per cent with a range of 5-9 wt. per cent.

#### **Flux Material**

A number of workers (e.g., Gasparik : 1983, Gasparik & Newton : 1984) have successfully used PbO flux to catalyze cation exchange reactions between silicates. However, because of its relatively high melting temperature, the use of PbO as a flux material had to be essentially limited above 1200°C in high P-T experimental studies. In this work, we have used a mixture of PbO and PbF<sub>2</sub> as flux material. Unfortunately, there are no data on the melting behavior of this mixture under high pressure. The 1 bar binary phase diagram (Sandolini : 1914, quoted in Levin et al., 1964) shows the eutectic point for the system at about 490°C (compared to 888°C for the melting of pure PbO). The results of a trial run with two flux compositions (0.75 PbF<sub>2</sub> and 0.55 PbF<sub>2</sub>) loaded separately with Gt-Opx mixtures within a graphite disk suggested 0.55 PbF<sub>2</sub> + 0.45 PbO to be a relatively effective flux composition at the high P-T conditions of these experiments.

The effectiveness of PbO-PbF<sub>2</sub> flux in promoting Fe-Mg exchange between garnet and orthopyroxene is clearly demonstrated by a run at 30 Kb, 1200°C for 2 days. A small portion of a Gt-Opx mixture was mixed with the flux and packed inside one of the sample holes of a two-hole graphite disk, the other hole containing a portion of the same mixture, but without the flux. As illustrated in Fig. 4, the products of the fluxed run showed a significantly larger shift of composition toward equilibrium.

The PbO-PbF<sub>2</sub> flux was found to melt substantially in the lowest temperature experiment, 750°C at 20 Kb, attempted in this work. However, we failed to get an adequate exchange reaction below 975°C. Part of the flux was usually converted to Pb by reaction with graphite capsule. As Pb has a relatively lower melting temperature (Akella et al., 1973), the reduction of PbO to Pb should promote melting of the flux. As shown in Fig. 2, the flux dissolved a substantial portion of the initial sample (40-60 per cent), and the residual material sank to the bottom of the graphite container. Microprobe analyses of the glassy material near the top of the container showed Pb, F, Fe, Mg, Ca, Al, Si, Cs, and Cl, the last two elements being derived from the insulation CsCl sleeve around graphite furnace of the pressure cell. The substitution of Pb and F within the silicates in all run products was found to be limited to 0.1~0.3 wt. percent, which is

too dilute to have any significant effect on the equilibrium compositions of coexisting garnet and orthopyroxene.

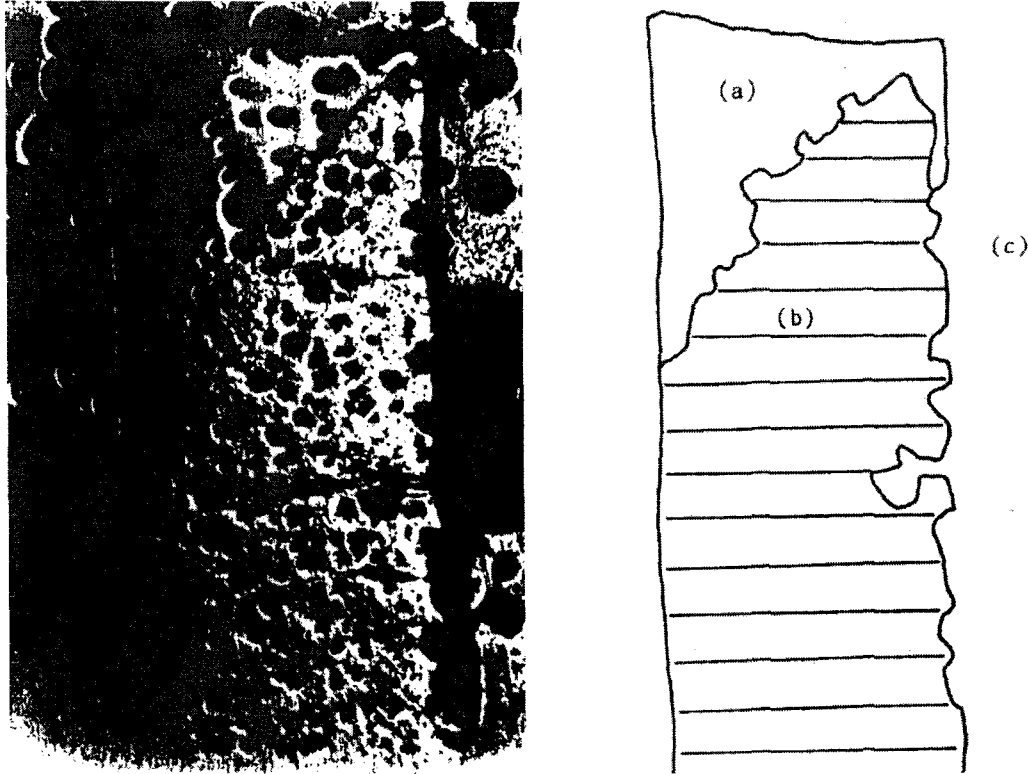


Fig. 2 Cross section of fluxed run product at 975°C, 20Kb. Top portion(a) represents glass including various constituents of starting material eg. Fe, Mg, Si, Al, pressure medium ie. Cs, Cl and flux material eg. Pb, F. Bottom portion(b) is composed of equilibrated crystals of garnet and orthopyroxene that sank through the molten flux. Surrounding the sample we have epoxy(c), which was used to mount the sample.

Owing to the dissolution of the sample in the flux, the choice of the optimal flux to sample ratio that would promote adequate reaction, but at the same time retain enough undissolved sample for microprobe analysis, appeared to be a tricky problem. In several runs, the entire samples were dissolved in the flux. The flux to sample ratio in the successful runs are shown in Table 2.

#### Analytical Method

The run products were analyzed with an automated ARL scanning electron microprobe using a 15 KV accelerating voltage and a 25mA sample current. The X-ray intensity and background for each measurement was corrected automatically by the computer program Task II(McCarthy, 1975) and the analytical data were reduced by the Bence-Albee method (Bence & Albee, 1968). Instrumental drift was handled by recalibrating at approximately 3 hour intervals. The standards used were as follows : anorthite for Al and Ca, diopside for Mg and Si, fayalite for Fe, rhodonite for Mn, albite for Na, chromite for Cr, sphene for Ti, and orthoclase for K.

Only those analyses which had total wt. per cent oxide between 99 and 101, and satisfied the theoretical stoichiometry of the mineral within 2 per cent, were considered acceptable for the

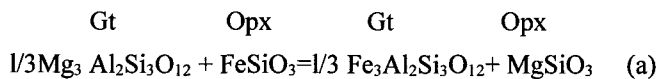
determination of  $K_D$ . All iron was assumed to be in the ferrous state. (Calculations of  $f_{O_2}$  condition in the C-O<sub>2</sub> system in the presence of graphite suggests that for values at the run conditions were between those defined by QFM and WI buffers, and within  $\pm 2$  log units of the WM buffer. The  $f_{O_2}$  for the C-H<sub>2</sub>O +graphite system lies between those of C-O<sub>2</sub>+ graphite system and WI buffer.)

**EXPERIMENTAL RESULTS AND THERMO-DYNAMIC ANALYSIS**

The run data are summarized in Table 2, and the compositions of coexisting garnet and orthopyroxene at selected P-T(nominal) conditions are illustrated in Fig. 4. Fig. 3 is structure of run product illustrating the shape and size of mineral grains. Generally the grain size of orthopyroxene was small, which caused major problems during microprobe analyses and resulted in numerous analyses which were unacceptable in terms of the criteria discussed earlier. Both garnet and orthopyroxene usually displayed significant compositional inhomogeneities. Consequently, equilibrium compositions of coexisting garnet and orthopyroxene were determined on the basis of microprobe analyses made as close to their mutual contacts as possible, but without introducing 'edge' effects(El-phick, et al. : 1985, Ganguly, et al. : 1987).

Nominal* T °C	Time P, Kb	Time hrs	Starting mixture	Flux/sample wt. ratio	Initial $K_D$	Resultst		
						$X_{Fe}^{Gt}$	$X_{Fe}^{OPx}$	Final $K_D$
975±5	20±0.5	168	Opx/ 4, Gt/2	0.80	∞	0.44	0.26	2.17
			Opx/ 1, Gt/2	0.80	6.36	0.49	0.31	2.14
			Opx/ 1, Gt/1	0.80	2.41	0.56	0.37	2.21
			Opx/ 4, Gt/1	0.80	∞	0.58	0.38	2.24
			Opx/ 2, Gt/1	0.80	0.72	0.91	0.83	2.23
1050±5	26±1	168	Opx/ 3, Gt/3	0.80	0.00	0.36	0.21	2.12
			Opx/ 1, Gt/2	0.80	6.36	0.42	0.27	1.97
			Opx/ 1, Gt/1	0.80	2.41	0.53	0.34	2.15
1100±10	25±0.5	61	Opx/ 1, Gt/1	0.10	2.41	0.55	0.37	2.06
			Opx/ 2, Gt/1	0.10	0.72	0.79	0.65	2.02
1200±5	26±1	120	Opx/ 4, Gt/2	0.10	∞	0.22	0.13	1.83
			Opx/ 1, Gt/2	0.10	6.36	0.44	0.30	1.80
			Opx/ 1, Gt/2	0.10	6.36	0.40	0.25	1.96
			Opx/ 3, Gt/3	0.10	0.00	0.34	0.22	1.89
			Opx/ 3, Gt/3	0.10	0.00	0.24	0.15	1.77
1200±10	25.5±0.5	55	Opx/ 1, Gt/2	0.05	2.41	0.64	0.47	1.98
1200±10	32.5±1.5	48	Opx/ 2, Gt/1	0.05	0.72	0.84	0.74	1.83
1300±10	37.5±0.5	24	Opx/ 1, Gt/1	0.05	2.41	0.46	0.32	1.76
1300±5	39.5±0.5	48	Opx/ 2, Gt/1	0.00	0.72	0.81	0.70	1.80
1400±5	45.5±0.5	24	Opx/ 1, Gt/1	0.00	2.41	0.55	0.43	1.60
1400±5	43.5±0.5	45	Opx/ 2, Gt/2	0.00	0.19	0.61	0.48	1.64
1400±5	43.5±0.5	45	Opx/ 5, Gt/2	0.00	0.68	0.63	0.51	1.60

The Fe<sup>2+</sup>-Mg fractionation between garnet and orthopyroxene can be treated in terms of the following exchange equilibrium



Thus, at equilibrium

$$K(a) = \left[ \frac{X_{Fe}^{Gt} X_{Mg}^{Opx}}{X_{Mg}^{Gt} X_{Fe}^{Opx}} \right] \cdot \left[ \frac{\gamma_{Fe}^{Gt} \gamma_{Mg}^{Opx}}{\gamma_{Mg}^{Gt} \gamma_{Fe}^{Opx}} \right] = \left[ \frac{(Fe/Mg)^{Gt}}{(Fe/Mg)^{Opx}} \right] \cdot \left[ \frac{(\gamma_{Fe}/\gamma_{Mg})^{Gt}}{(\gamma_{Fe}/\gamma_{Mg})^{Opx}} \right] \quad (1)$$

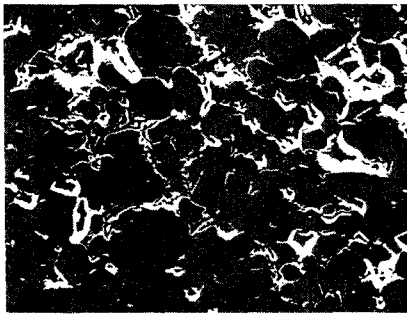


Figure 3-a

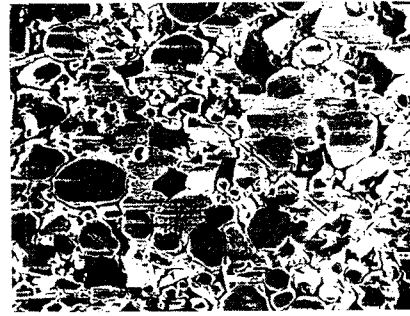


Figure 3-b

Fig. 3 Experimental run products. Horizontal bar=20 $\mu$ m. Garnets are equant with rounded margins, and orthopyroxene grains are subhedral, elongated and prismatic. Photos were taken using the backscattered electron signal and raster scan capabilities of the microprobe.  
 Fig. 3-a : 1400 $^{\circ}$ C, 45Kb  
 Fig. 3-b : 1300 $^{\circ}$ C, 35Kb

where  $K(a)$  is the equilibrium constant of reaction (a), and  $\gamma$  is the activity coefficient of the specified endmember component on a one-cation basis. We define the quantities within the first and second square brackets as  $K_D$ (distribution coefficient) and  $K_D$ , respectively.

The data presented in Fig. 4 suggest the  $K_D$  to be essentially independent of Fe/Mg ratio at  $T > 975^{\circ}\text{C}$ . This conclusion is corroborated by the extensive data of Kawasaki &

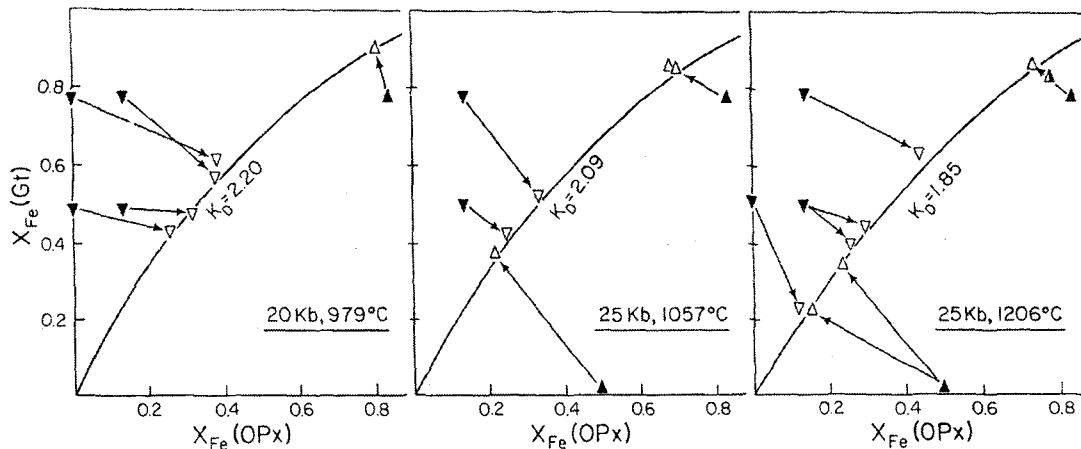


Fig. 4 Fractionation of Fe and Mg between coexisting garnet and orthopyroxene at selected P-T (nominal) conditions,  $X_{\text{Fe}} = \text{Fe}/(\text{Fe} + \text{Mg})$ . See Table 2 for correction of nominal temperatures. All Fe is assumed to be divalent. Solid triangles; starting composition; half-filled and open triangles: final compositions in dry run and in runs made with PbO-PbF<sub>2</sub> flux, respectively; arrows: direction of evolution of compositions. The development of two different final compositions from the same starting composition at 25Kb, 1200 $^{\circ}$ C is a consequence of different Gt/OPX ratios. All runs were in graphite capsules.

Matsui(1983, Fig.6) at 1100 $^{\circ}$ C and 1300 $^{\circ}$ C. The simplest explanation for this lack of compositional dependence of  $K_{\text{rj}}$  is that Fe and Mg mix essentially ideally in both garnet and orthopyroxene at  $T > 975^{\circ}\text{C}$  or that the nonideal Fe-Mg interactions in the two minerals effectively compensate for one another at  $T \geq 975^{\circ}\text{C}$ . We can, thus reduce the polybaric Fe-Mg fractionation data to an arbitrary isobaric condition of 25 Kb as follows

$$\left(\frac{\partial \ln K_D}{\partial p}\right)_T = \left(\frac{\partial \ln K}{\partial p}\right)_T = \frac{-\Delta V^\circ}{RT} \quad (2.1)$$

$$\ln K_D(25\text{Kb}, T) = \ln K_D(P, T) - \int_P^{25\text{Kb}} \frac{\Delta V^\circ}{RT} dp \quad (2.2)$$

The last term in (2.2) is integrated by assuming  $\Delta V^\circ$  to be independent of pressure in the range of pressure(20 to 45 kb) of these experiments. The error introduced by this assumption is small compared to the uncertainty of the experimental and volumetric data.

The molar volumes for the pure end members are taken from the measurements on synthetic samples by Charlu et al. (1975), Takahashi & Kushiro(1983), and Chatillon-Cohnet et al.(1983a, b) and shown in Table 3.

End member	$\Delta H_f^\circ$ (Kcal/mole)	$\Delta S_f^\circ$ (e. u.)	Cp Coefficients (cal/mole)			V* (cm <sup>3</sup> /mole)	References
			a	b × 10 <sup>3</sup>	c × 10 <sup>-1</sup>		
Pyrope (1/3Mg <sub>3</sub> Al <sub>2</sub> Si <sub>2</sub> O <sub>11</sub> )	-508.669 <sup>b</sup>	21.03 <sup>b</sup>	35.46	4.02	9.69 <sup>b</sup>	37.756 <sup>d</sup>	a) Takahashi & Liu (1970) b) Saxena & Erikson (1983)
Almandine (1/3Fe <sub>3</sub> Al <sub>2</sub> Si <sub>2</sub> O <sub>11</sub> )	-423.008 <sup>a</sup>	22.82 <sup>b</sup>	32.51	11.23	6.24 (≤848°K) <sup>b</sup>	38.483 <sup>d</sup>	
Enstatite (MgSiO <sub>3</sub> )	-369.962 <sup>b</sup>	15.83 <sup>b</sup>	35.69	7.41	3.54 (≥848°K)	31.31 <sup>c</sup>	c) Charlu et al. (1975)
Ferrosilite (FeSiO <sub>3</sub> )	-285.494 <sup>a</sup>	22.60 <sup>b</sup>	27.72	3.48	9.79 <sup>b</sup>	32.99 <sup>d</sup>	d) Chatillon Colinet et al. (1983)

$\Delta H_f^\circ$  and  $\Delta S_f^\circ$  are for formation from oxides at 1 atm., 298°K; molar volume (V\*) is at 1 atm., 298°K; Cp = a + bT - c/T<sup>2</sup>

Linear least squared fit of the reduced isobaric  $\ln K_D$  data versus 1/T yields the following relation(r = 0.96)

$$\ln K_D(25\text{Kb}) = \frac{2269(\pm 142)}{T(\text{K})} - 0.96 \quad (3.1)$$

or, using(2.2),

$$\ln K_D = \frac{1971(\pm 166) + 11.9 P(\text{Kb})}{T(\text{K})} - 0.96 \quad (3.2)$$

where the uncertainties represent one  $\sigma$  value. All 23  $K_D$  values, obtainable from table 2, have been used for the regression. The expression (3.2) yields a value of  $^{\wedge}\Delta H^\circ_a$  of -3916(±282) cal. at 1 bar, 975-140 0°C.

Fig.5 shows a conventional plot of  $\ln K_D$  vs. 1/T according to the regressed expression (3.1), along with the experimental data. We performed an additional experiment at 20Kb, 750°C with PbO-PbF<sub>2</sub> for one week to constrain the low temperature exchange equilibrium. However, it failed to yield any significant reaction between garnet and orthopyroxene even though the flux was molten in the charge.

Fig. 6 shows a comparison of our results on the temperature dependence of  $\ln K_{rj}$  with the experimental results of Kawasaki and Matsui(1983) and Harley(1984) in the FMAS system, and the theoretical deductions of Sen and Bhattacharya(1984). All data are normalized to 25Kb. The various experimental



results agree within the limits of their uncertainties. However, the best fit to Harley's data lies about 70-85°C lower than that to our data.

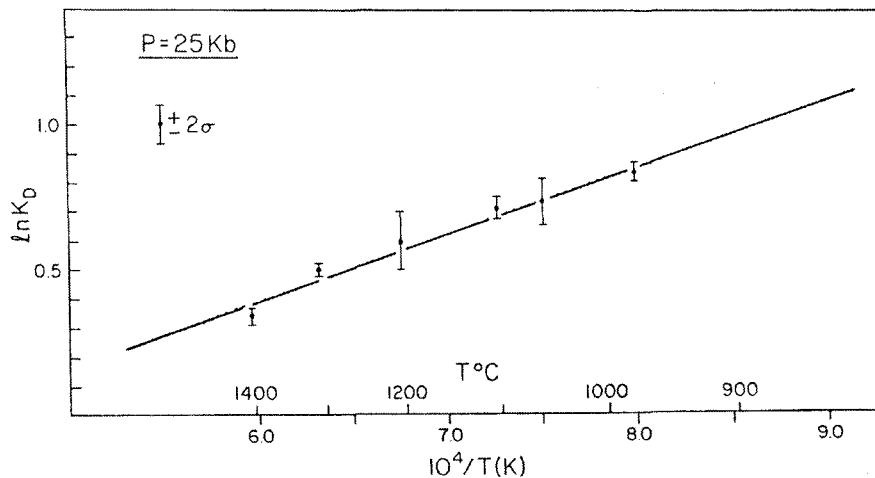


Fig. 5  $\ln K_D$  versus reciprocal temperature. The data with vertical bars represent mean with  $2\sigma$  uncertainty of the reversed experimental determinations in the FMAS system. All data are normalized to 25 Kbar. The solid line represent least squared fits to all (23) experimental data according to the assumptions of  $\Delta C_p=0$

Harley(1984) performed some of his experiments in Fe capsules, and noted substantial iron addition to the charge from the encapsulating material. He revised the  $\ln K_D$  values upward by 0.15-0.20 units on the basis of the observation that the run "in graphite capsules with mixes not susceptible to Fe addition" yielded  $\ln K_D$  values greater by the above magnitude compared to those made in Fe capsule. The  $K_D$  values obtained through these arbitrary adjustments may not be very precise. Further, the data shown in Fig. 4 and those of Kawasaki and Matsui(1983: Fig.4) do not suggest any significant dependence of  $K_D$  on Fe/Mg ratio at the temperatures of Harley's experiments.

In Sen and Bhattacharya's(1984) formulation,  $k_d$  depends on Fe/Mg ratio. In view of the experimental data, discussed above, suggesting lack of any significant effect on Fe/Mg ratio on  $K_D$  at  $T \geq 975^\circ\text{C}$ , we have ignored the Fe-Mg nonideality term in their formulation to compare it with the experimental data. Dependence of  $K_D$  on Fe/Mg ratio can not be ruled out at lower temperatures, but correction for this effect has to await further experimental Fe-Mg fractionation and/or mixing property data at lower temperatures.

## DEVELOPMENT OF GARNET-ORTHOPIROXENE GEOTHERMOMETER

The application of the Fe-Mg fractionation data to the geothermometry of natural assemblages obviously requires correction for the effects of additional components which can substitute significantly in garnet and orthopyroxene solid solutions. The major substitutional cations in natural assemblages are Ca, Mn, and  $\text{Cr}^{+3}$ . The last one is relatively unimportant in crustal assemblages, but may have significant effect in mantle xenoliths (Wood and Nicholls, 1978).

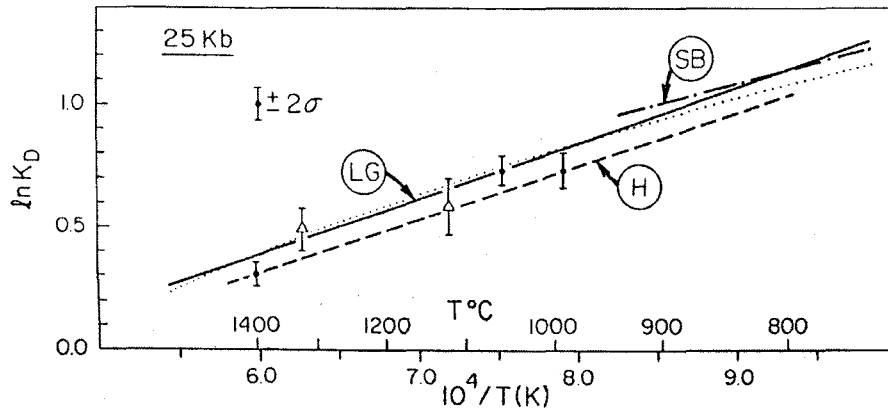


Fig. 6 Comparison of the  $\ln K_D$  vs  $1/T$  relation determined in this work (LG : solid line) with the experimental determinations of Kawasaki and Matsui (1983), shown by triangles, and Harley (1983), and the theoretical calibration of Sen & Bhat-tacharya (1984), neglecting their Fe Mg nonideality term.

Mn and Ca substitute highly preferentially in garnet relative to coexisting orthopyroxene (e.g. Dahl, 1980). Consequently, the effect of possible nonideal interactions of Mn and Ca in orthopyroxene of  $k_D$  is usually expected to be negligible compared to those in garnet, especially in the range of compositions of common natural assemblages. Following the multi-component simple mixture model of Ganguly and Kennedy (1974) for the quaternary garnet solid solution  $(\text{Fe, Mg, Ca, Mn})_3\text{Al}_2\text{Si}_3\text{O}_{12}$

$$RT \ln(\gamma_{\text{Fe}} / \gamma_{\text{Mg}})^{\text{Gt}} = W_{\text{FeMg}}^{\text{Gt}} (X_{\text{Mg}} - X_{\text{Fe}})^{\text{Gt}} + (W_{\text{FeCa}} - W_{\text{MgCa}})^{\text{Gt}} X_{\text{Ca}}^{\text{Gt}} + (W_{\text{FeMn}} - W_{\text{MgMn}})^{\text{Gt}} X_{\text{Mn}}^{\text{Gt}} \quad (4)$$

where  $W_{ij}$  indicates a 'simple mixture' interaction parameter between  $i$  and  $j$  components, as defined by Guggenheim (1967). In eqn. 4,  $W_{\text{FeMg}}^{\text{Gt}}$  becomes zero since Fe and Mg in both garnet and orthopyroxene are assumed to mix ideally at  $T \geq 975^\circ\text{C}$ . Thus,  $K_D$  in reaction (a) can be expressed as follows

$$RT \ln K_D = -\Delta W_{Ca}^{Gt} \cdot X_{Ca}^{Gt} - \Delta W_{Mn}^{Gt} \cdot X_{Mn}^{Gt} \quad (5)$$

where  $\Delta W_{Ca}^{Gt}$  and  $\Delta W_{Mn}^{Gt}$  indicate  $(W_{MgCa} - W_{FeCa})^{Gt}$  and  $(W_{MgMn} - W_{FeMn})^{Gt}$  respectively and according to Ganguly and Saxena (1984),  $\Delta W_{Ca} = \Delta W_{Mn} = 3000(\pm 500)$  calories per mole of cation for  $X_{Ca}^{Gt} \geq 0.30$  and  $X_{Mn}^{Gt} \geq 0.30$ . Using relation of  $\ln K_D = \ln K - \ln K_D \gamma$  in eqn. 1, we can recast (3.2) and (5) into the following geothermometric expression

$$T = \frac{1971 + 11.91P + 1510(X_{Ca} + X_{Mn})^{Gt}}{\ln K_D + 0.96} \quad (6)$$

where T is in K and P is in Kb.

The assumption of the independence of  $K_D$  on Fe/Mg ratios, which has been used to develop the geothermometric expression above, is well justified by our experimental data and those of Kawasaki and Matsui (1983) for  $T \geq 975^\circ\text{C}$  (that is for most assemblages in mantle derived xenoliths), but may not be valid at significantly lower temperature. Thus, the application of the geothermometer to granulite facies assemblages should be made caution.

We do not, as yet, have adequate mixing property data to correct for the effect of  $\text{Cr}^{+3}$ . However, substitution of  $\text{Cr}^{+3}$  in garnet would still affect  $K_D$  (see Wood & Nicholls, 1978). Thus, the above geothermometric expression may not yield reliable temperature for  $\text{Cr}^{+3}$  rich composition

## REFERENCES

- Akella, J., & Boyd, F.R. (1973) Effect of pressure on the composition of coexisting pyroxene and garnet in the system  $\text{CaSiO}_3 - \text{MgSiO}_3 - \text{FeSiO}_3 - \text{CaAlTi}_2\text{O}_6$ . *Carnegie Inst. Wash. Yearb.*, v. 72, p. 523-526
- Bence, A.E., & Albee, A.L. (1968) Empirical correction factors for the electron microanalysis of silicate and oxides. *J. Geol.*, v. 67, p. 382-403.
- Boettcher, A.L., Windom, K.E., Bohlen, S.R., & Luth, R.W. (1981) Low-friction anhydrous low to high-temperature furnace assembly for piston cylinder apparatus. *Rev. Sci. Instrum.*, v. 52, p. 903-1904
- Charlu, T.V., Newton, R. C., & Kleppa, O.J. (1975) Enthalpies of formation at 970 K of compounds in the system  $\text{MgO} - \text{Al}_2\text{O}_3 - \text{SiO}_2$  from high temperature solution calorimetry. *Gochim. Acta*, v. 39, p. 1487-1497
- Chatillon-Colinet, C., Kleppa, O.J., Newton, R.C., & Perkins, D. (1983a) Enthalpy of formation of  $\text{Fe}_3\text{Al}_2\text{Si}_3\text{O}_{12}$  (almandine) by high temperature alkali borate solution calorimetry. *Geochim. Cosmochim. Acta*, v. 47, p. 439-444
- Chatillon-Colinet, C., Newton, R.C., & Perkins, D. & Kleppa, O. J. (1983b) Thermochemistry of  $(\text{Fe}^{2+}, \text{Mg})\text{SiO}_3$  orthopyroxene. *Geochim. Cosmochim. Acta*, v. 47, p. 1597-1603
- Dahl, P.S. (1980) The thermal-compositional dependence of Fe-Mg distributions between coexisting

- garnet and pyroxene : Application to geothermometry. *Ame. Mineral.*, v. 65, p. 854-866.
- Elphick, S.C., Ganguly, J., & Loomis, T. P. (1985) Experimental determination of cation diffusivities in aluminosilicate garnets ; I. Experimental methods and interdiffusion data. *Contr. Miner. Petrol.*, v. 30, p. 36-44
- Harley, S. L. (1984) An experimental study of the partitioning of Fe and Mg between garnet and orthopyroxene. *Contr. Miner. petrol.*, v. 86, p. 359-373
- Kawasaki, T., & matsui, Y. (1977) Partitioning of Fe and Mg between olivine and garnet. *Earth Planet. Sci. Let.*, v. 37, p. 159-166
- Kawasaki, T., & matsui, Y. (1983) Thermodynamic analyses of equilibria involving olivine, orthopyroxene and garnet. *Geochim. Cosmochim. Acta*, v. 47, p. 1661-1679
- Lane, D.L., & Ganguly, J. (1980) Al<sub>2</sub>O<sub>3</sub> solubility in orthopyroxene in the system MgO - Al<sub>2</sub>O<sub>3</sub> - SiO<sub>2</sub> : A reevaluation, and mantle geotherm. *J. Geophys. Res.*, v. 85, p. 6963-6972.
- McCarthy, J. (1975) Wave dispersive spectrometer and stage sutomation program. NS-892. Tracor-Northern, Inc., Middleton, WI.
- Mirwald, P.W., Getting, I.C., & Denedy, G.C. (1975) Low friction cell for piston-cylinder high pressure appatatus. *J. Geophys. Res.*, v. 80, p. 1519-1525
- Sen, S.K., & Bhattacharya, A. (1984) An orthopyroxene-garnet thermometer and its application to the Madras charnockites. *Contr. Miner. Petrol.*, v. 88, p. 64-71
- Wood, B.J., & Nicholls, J. (1978) The thermodynamic properties of reciprocal solid solutons. *contr. Miner. Petrol.*, v. 66, p. 389-400